SUPPLEMENTARY INFORMATION

Conformationally Selective RNA Aptamers Allosterically Modulate the β_2-Adrenoceptor

Alem W. Kahsai[1], James W. Wisler[1], Jungmin Lee[1,7], Seungkirl Ahn[1], Thomas J. Cahill III[1,2], S. Moses Dennison[5], Dean P. Staus[1], Alex R. B. Thomsen[1], Kara M. Anasti[5], Biswaranjan Pani[1], Laura M. Wingler[1], Hemant Desai[9], Kristin M. Bompiani[3,4,11], Ryan T. Strachan[8], Xiaoxia Qin[10], S. Munir Alam[5], Bruce A. Sullenger[3,4], and Robert J. Lefkowitz[1,2,6,*]

Departments of [1]Medicine, [2]Biochemistry,and [3]Surgery, and [4]Duke Translational Research Institute, [5]Duke Human Vaccine Institute and the [6]Howard Hughes Medical Institute, Duke University Medical Center, Durham, NC, 27710

[7]Department of Chemistry and Chemical Biology, Harvard University, Cambridge, MA 02138

[8]Department of Pharmacology, [9]The University of North Carolina School of Medicine, Chapel Hill, NC 27516

[10]Genome Sequencing and Analysis Core Resource, Duke University, Durham, NC, 27710

[11]The University of California, San Diego, Moores Cancer Center, La Jolla, CA 92093

[*]Correspondence and requests for materials should be addressed to R.J.L. (lefko001@receptor-biol.duke.edu)

SUPPLEMENTARY RESULTS

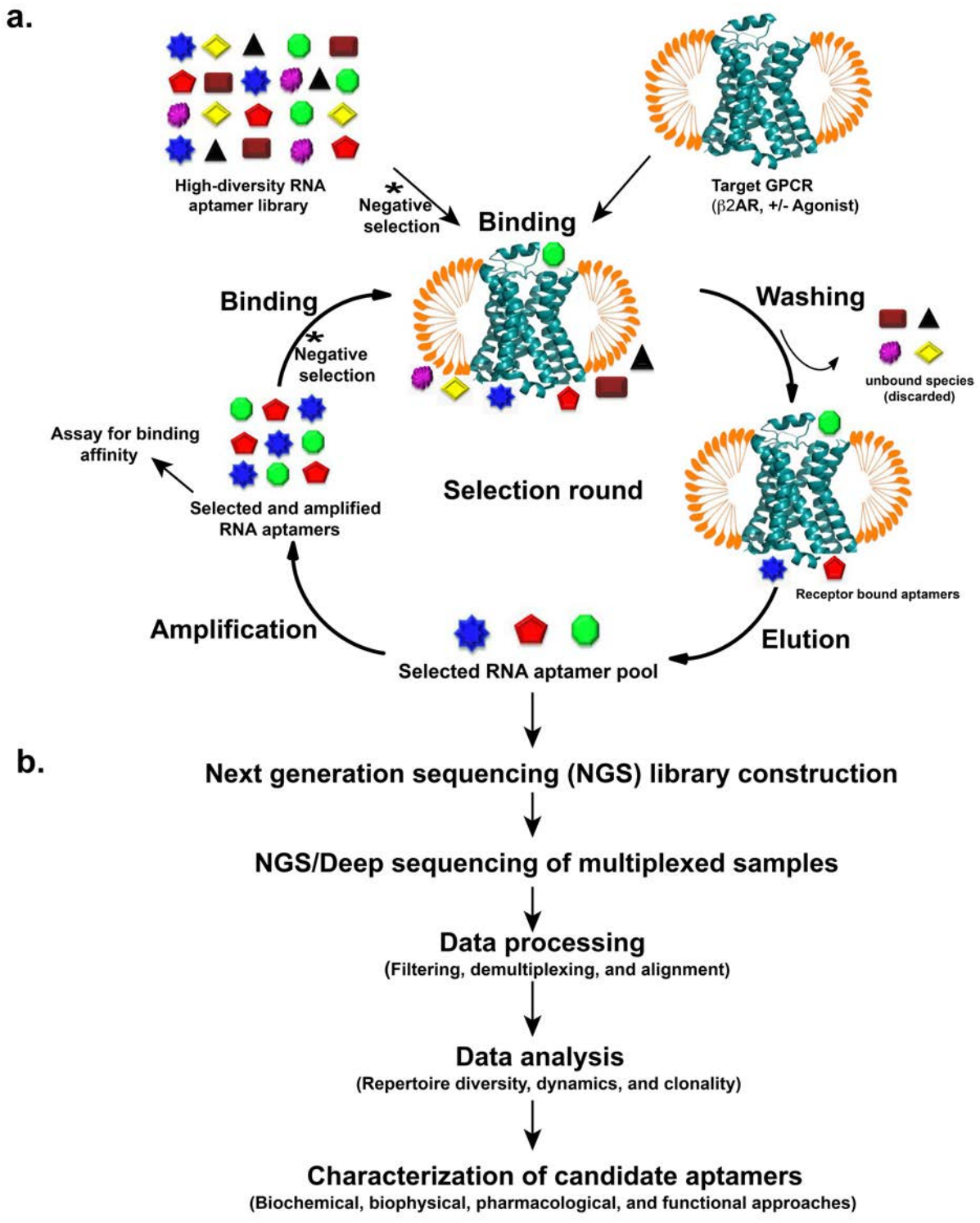

Supplementary Figure 1: Schematic illustration of the selection strategy and NGS analysis to generate conformation-specific RNA aptamers against the β_2AR. (**a**) Scheme of the RNA aptamer SELEX procedure using 2'-F-pyrimidine modified RNA library. The library consisted of 80 nucleotide-long single-stranded RNA oligonucleotides with a central random region of 40 nucleotides, flanked by constant regions of a 15-base 5′-primer sequence and a 25-base 3′-primer

sequence. Prior to the addition of the protein target, negative (or counter) selection steps (indicated by asterisk in black) are done to remove RNA molecules that bind nonspecifically to selection matrix such as nitrocellulose membrane filter and other components of the selection media. In the binding step, the pre-cleared RNA pool is incubated with the target protein, unliganded or BI167107-bound-β2AR. Following washing procedures to remove unbound RNA species, RNA:protein complexes are recovered by elution, amplified by a combination of reverse transcription, PCR, and *in vitro* transcription; and used as a new enriched RNA pool for the next round of selection. Binding assay (such as double filter based) is performed to monitor the progress of selection after each SELEX round by measuring the affinity of the radiolabeled-enriched RNA pools for the targets. (**b**) Next generation sequencing (NGS) of RNA aptamer pools. After enriching for RNA aptamers, herein in after nine rounds of selection, the RT-PCR products that were amplified are used to construct libraries for multiplex applications and generate next generation sequencing libraries (HiSeq 2000 by Illumina, Inc; Duke Center for Genomic and Computational Biology, Duke University). After high-throughput next-generation DNA sequencing, the resulting data are prepared for bioinformatics analysis. Target binding candidate aptamers are later characterized using biochemical, functional, biophysical, and structural techniques.

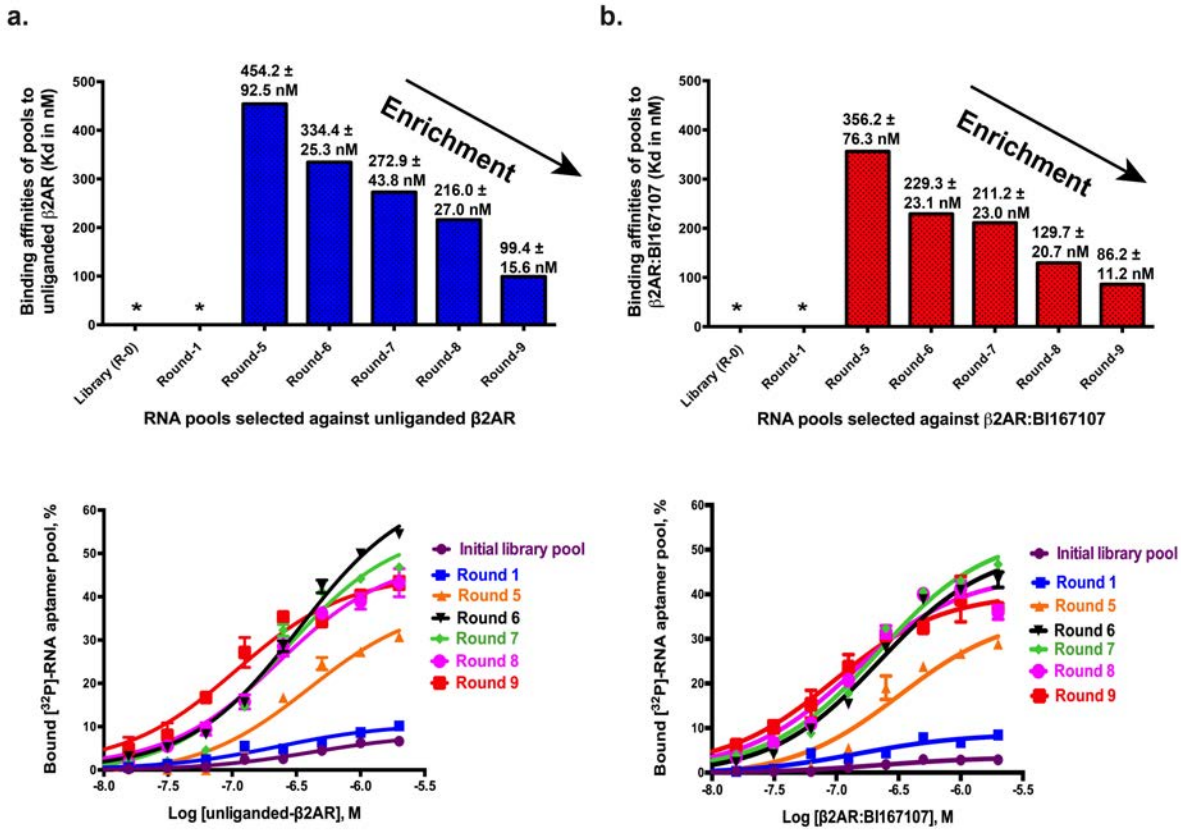

Supplementary Figure 2: Monitoring of enrichment of selection process by binding assay of successive rounds of radiolabeled RNA pools with unliganded or BI167107-bound-β_2AR. (**a**,**b**) The binding ability of the starting naïve library (R0) and selected RNA pools (R1, R5, R6, R7, R8, and R9) for unliganded or BI167107-bound-β_2AR were analyzed by filter binding assay as described in methods. Each individual RNA pool was 5′-end ^{32}P-labelled and incubated with

increasing amounts of β_2AR concentrations (as unliganded or BI167107-bound form). The percentage of input RNA retained on the filter in β_2AR:RNA complexes were calculated to obtain values for bulk equilibrium dissociation constants (K_d) by fitting to one-site hyperbolic specific binding. Top panels, K_d determinations ± standard errors for RNA pools from R5 through R9 against unliganded-β_2AR (blue graphs in **a**) and BI167107-bound-β_2AR (red graphs in **b**) are shown in nM concentrations. Bottom panels, binding curve representations (in a semi-log format) of the RNA pools with unliganded (**a**) or BI167107-bound-β_2AR (**b**) are illustrated as percentage of the total RNA bound (*y*-axis). Data shown are means with standard error of experiments repeated twice. The enrichments observed in the last round did not change with additional rounds of selections. Asterisks denote that the equilibrium dissociation constants (K_d) could not be obtained reliably from these experiments for those RNA pools due to low levels of binding.

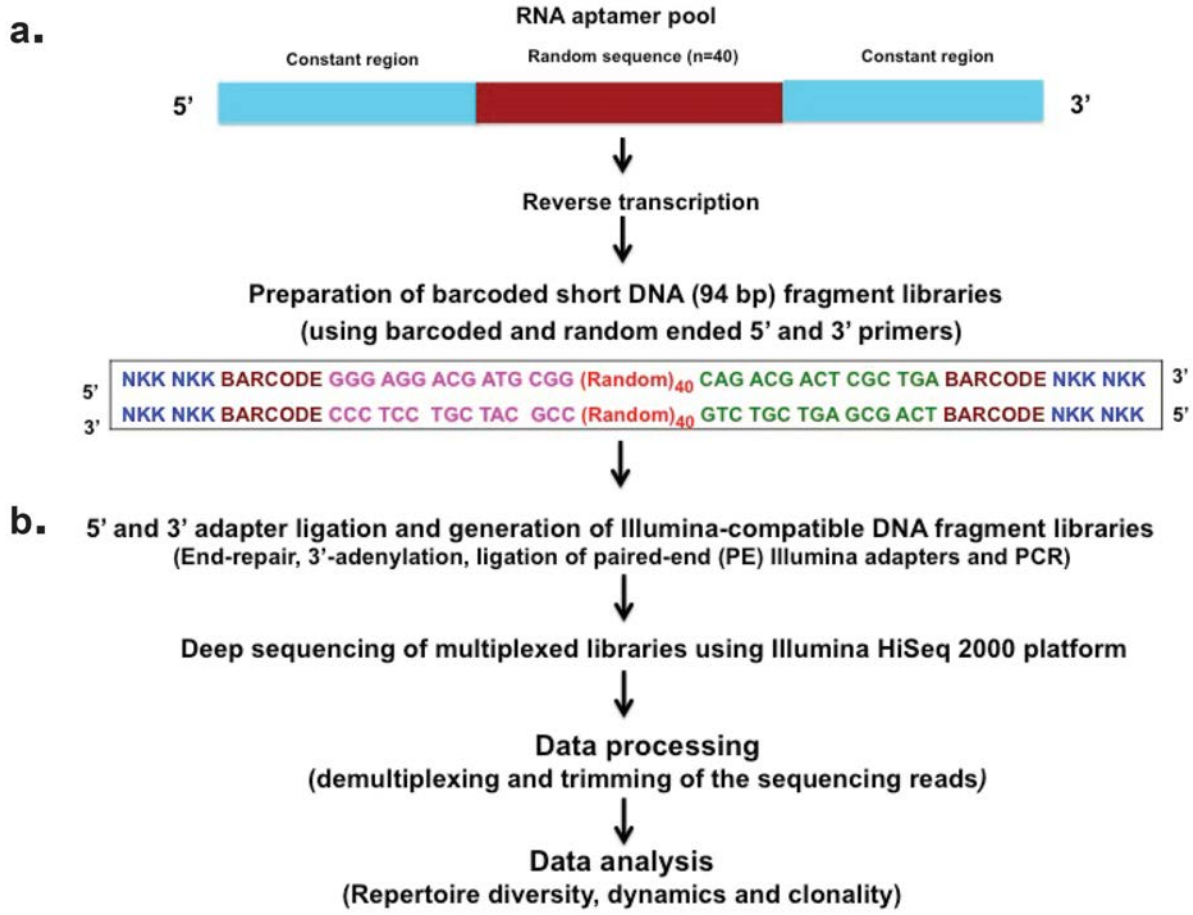

Supplementary Figure 3: Schematic presentation of library preparation and NGS analysis of selected RNA aptamer pools. (**a**) Each RNA pool is reverse transcribed and amplified via PCR to generate barcoded short DNA (94 bp long) fragment libraries. The 5' and 3' primers used to generate the DNA fragments by PCR contain NKKNKK region (colored in blue), which facilitates formation of clusters during Illumina sequencing; a 6-bp barcode region (colored in dark-red) for identifying each pool during multiplex sequencing; and 12-bases forward and reverse compliment sequences of the original variable region of the dsDNA PCR primers (colored in pink). The 40-bp long random region is shown in red. (**b**) Generation of

Illumina compatible DNA fragment libraries and high-throughput sequencing. DNA Fragments are converted into library by ligation to sequencing adapters containing specific sequences compatible with the Illumina NGS platform flow-cell by processes involving end-repair, 3′ adenylation, ligation of paired-end (PE) Illumina adapters and PCR. The next step involves amplification of the library by cluster generation and high-throughput sequencing from both ends of the library inserts (*i.e.,* paired end sequencing) on Illumina platform. Reads generated by high-throughput sequencing are identified through barcodes for each round pool, filtered, aligned and analyzed. Read frequencies, percent frequencies and fold-enrichment of each sequence are calculated and compared across multiple selection rounds.

a.

Apt ID	RNA aptamer sequence (5' – 3')	Affinity, K_d (in nM)		Fold-enrichment (R9/R4) for selection on	
		β2AR (Unliganded)	β2AR (Bound to BI)	β2AR (Unliganded)	β2AR (Bound to BI)
Apt 1	GCAUAACAGCUGGUCCACCGCCGCAUCAAGGCGAGAGCGC	746.4 ± 142.5	33.6 ± 7.0	32.0	113.1
Apt 2	GAUCCACCUGGAGGGGGUACAUCGCGCGGGUCGCCGAUUA	*	36.1 ± 19.2	129.5	794.9
Apt 3	UGUUGGGGCCGAACUAGUUCCGCGGGGACUAGUUGUGUGU	201.6 ± 33.4	181.7 ± 24.7	3.7	74.2
Apt 4	ACCACAGGGAGGAGGAGCCCGCCGCAUUUCUCGGACCCCG	*	*	35.9	371.0
Apt 5	ACUGCACGGAGGUGAGGGGGUAGUGGCACCGUCCACCCUA	*	*	400.5	1036.0
Apt 6	GCAAUCUGGCGUGGCCACGGAGGCUGCGGGGGCGCCAUGU	*	*	310.2	326.7
Apt 7	AAACGCUCGCGAGAGUACCGGCCUCCUUGGUUUAGCCCAC	331.0 ± 33.4	161.7 ± 79.1	1328.8	1823.1
Apt 8	GCUGUCGGGGGCACACGGAGGAGUGGGGGAUGCCUUUAUC	*	*	137.5	147.5
Apt 9	GACCCACCUGGAGGGGGUACAUCGCGCGGGUCGCCGAUUA	253.3 ± 233.1	48.1 ± 10.9	89.7	181.0
Apt 10	UCUGUAUGUGCUGUCGCCGAAGUUACAGCGUAUGCACUGU	304.9 ± 58.8	144.7 ± 46.7	3.4	0.1
Apt 11	UAGAUCUGCAGUAGUCAACGGAGGUGAGGGGAGACGUAAG	52.1 ± 13.9	72.4 ± 14.2	1241.8	1017.9
Apt 12	AUACACGAGGAGGAGCGUGCAUCCAGCUCUGAUUCUCAGU	562.8 ± 127.7	64.1 ± 7.9	92.7	3510.5
Apt 13	GUCUUAGCUCUGCAGCCCACGGAGGAGAGGGGAGGGCCGA	645.7 ± 121.5	37.3 ± 5.1	71.7	470.5
Apt 14	GCGUGUGUAUGUCGGAGCUGGUGUGUGAACCCAUUGGCUA	73.1 ± 39.0	74.0 ± 9.8	2.7	0.1
Apt 15	GUUGCCGUUCUGUCGUCACCAGCUUGACCAACGCGGUGUG	51.7 ± 7.8	115.7 ± 14.1	3.7	0.3
Apt 16	AACAAAGCAAGGAGGAGUGCUGCCGCAUUCUCGAAGGCCU	48.6 ± 10.3	*	739.7	248.8
Apt 17	CAAGGACAACUGCGCCCUAUCUCGGCACCGCUCAGCGCAU	*	179.0 ± 34.5	238.1	423.0
Apt 18	CUGUGUAGGAGGGACUAGCCGACUCCGAUCCGCGGUGGAG	668.2 ± 103.6	159.1 ± 20.5	387.8	5537.7
Apt 19	AAUCGGGCAAGUCCCGCUCUCAUCGUUCAGAACCAGGACC	165.6 ± 39.6	186.5 ± 15.6	67.1	1.5
Apt 20	GCCGUAAUCACCCGUGUGCCGCGGUAGCGUUCAUCGGUGU	56.0 ± 12.9	99.7 ± 25.4	9.0	3.0

b.

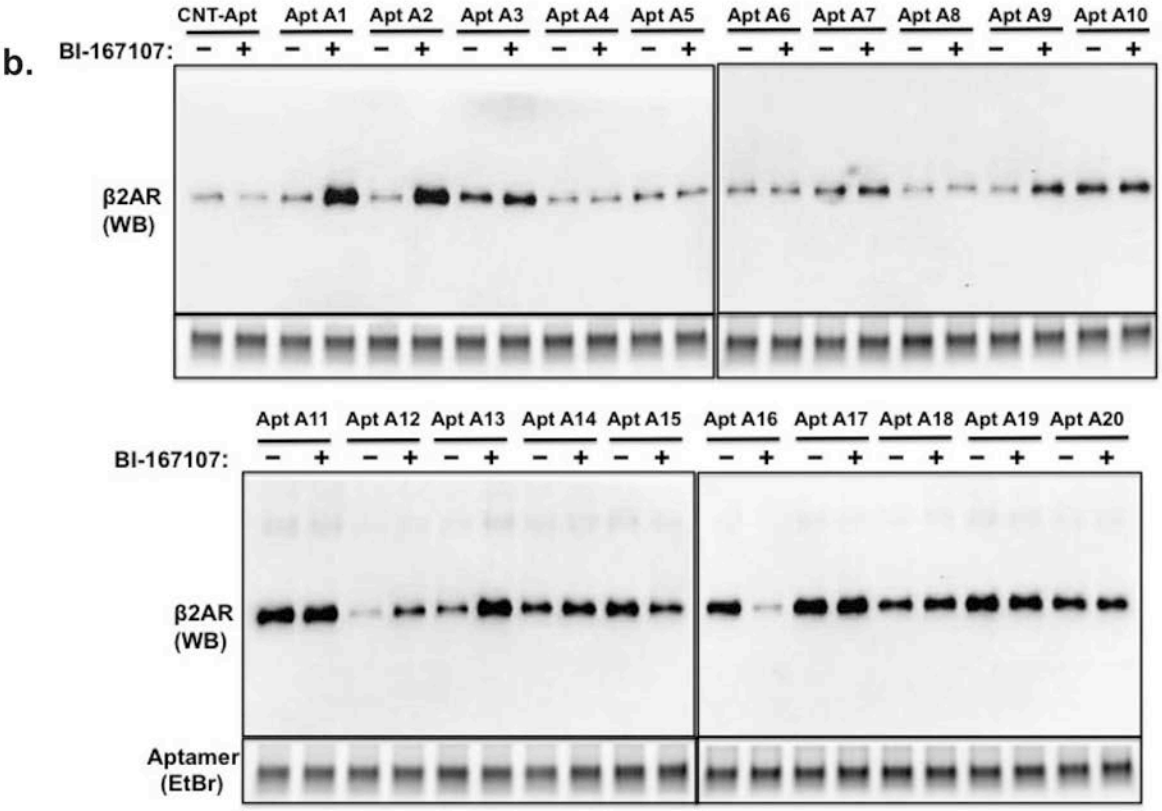

Supplementary Figure 4: Top 20 candidate aptamers from NGS analysis and their binding capacity to unliganded or BI167107-bound β_2AR. The binding capacity of 20 candidate aptamers to unliganded or BI167107-bound β_2AR as

evaluated by filter-binding and pull-down analyses. (**a**) The 40 base variable region (N = 40) for the top 20 candidate aptamers are shown. Equilibrium dissociation binding constants (K_d) measurements were performed with full-length (80-nucleotides long) molecules containing the flanking constant regions composed of a 15-base 5′-primer sequence and a 25-base 3′-primer sequence as described in methods. In the middle two columns, the affinity (K_d) of each aptamer for the unliganded and BI167107-bound forms of β_2AR are shown and were determined by nitrocellulose filter binding with the 5′-end ^{32}P-labelled aptamers and varying concentrations of the proteins. In the last two columns fold enrichment-ratios (R4 to R9) for each sequence are shown. Asterisks denote affinities were too low to be reliably determined due to poor signal to noise ratios under these experimental conditions. (**b**) Binding analysis illustrating the relative binding of the 5'-biotinylated forms of RNA aptamers for unliganded and BI167107-bound β_2AR in a pull-down assay. Neutravidin immobilized aptamers were incubated with β_2AR in absence or presence of agonist BI167107. β_2AR-biotin-aptamer complexes were eluted from the beads and analyzed by immunobloting to detect captured β_2AR and biotinylated-RNA aptamer as described in methods. Aptamers input are indicated by ethidium bromide staining of the eluted RNA. CNT-Apt denotes a non-binding control aptamer (with the 40-base variable region of 5′-GCUCCUACCGUAAAAACAGCGCCACAGCUACCCUUACUCA-3′). Boxed sequences indicate top binding RNA aptamers that demonstrated robust binding to β_2AR and/or have selectivity to either forms of β_2AR.

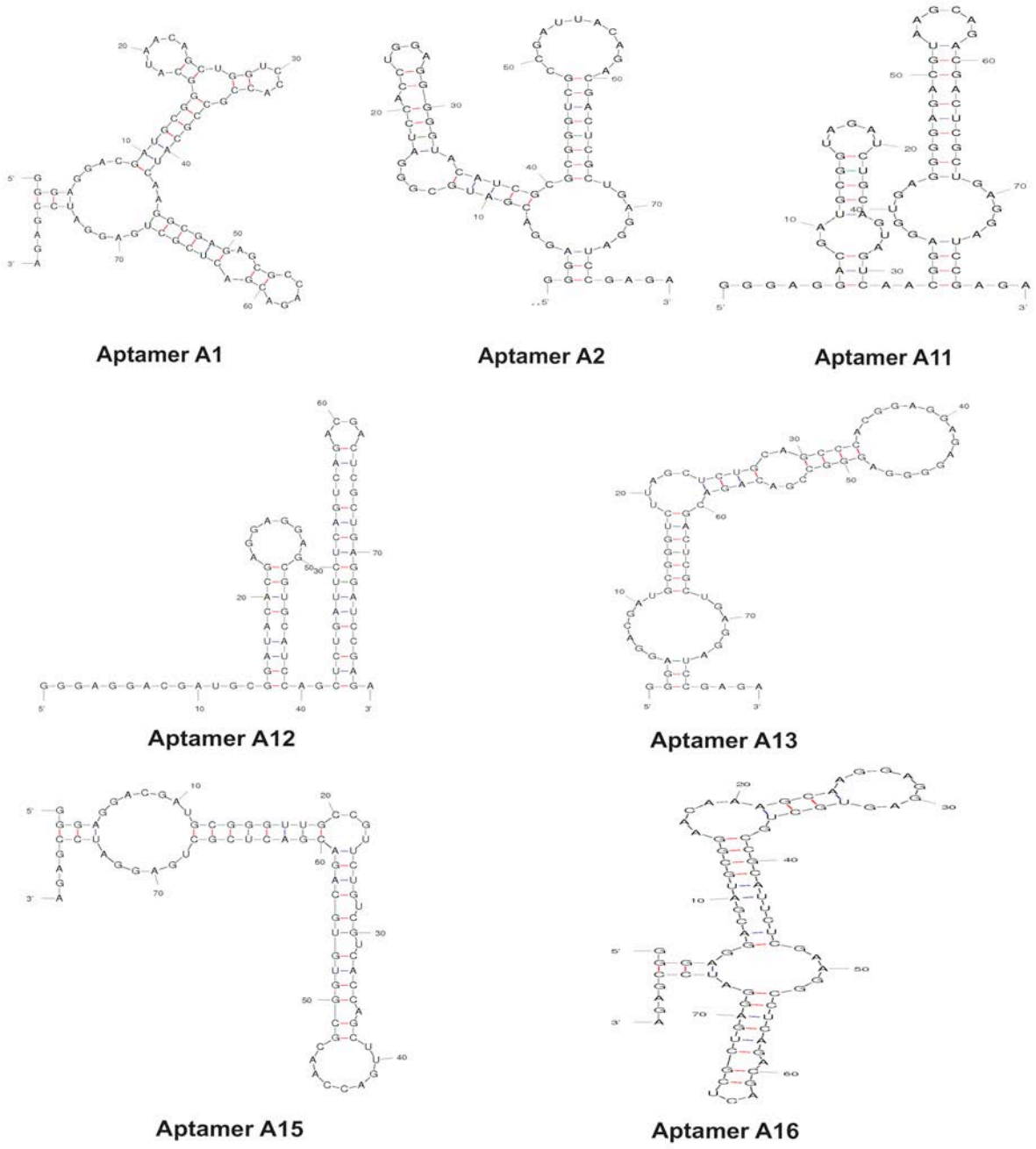

Supplementary Figure 5: Schematic representations of the secondary structures of the top 7 β_2AR binding RNA aptamers. Predicted secondary structures were generated by free energy minimization using the RNA folding algorithm Mfold (calculated free energy for each aptamer: ΔG_{A1} = -25.80 kcal/mol, ΔG_{A2} = -25.40 kcal/mol, ΔG_{A11} = -25.20 kcal/mol, ΔG_{A12} = -27.80 kcal/mol, ΔG_{A13} = -23.40 kcal/mol; ΔG_{A15} = -26.30 kcal/mol, and ΔG_{A16} = -26.0 kcal/mol).

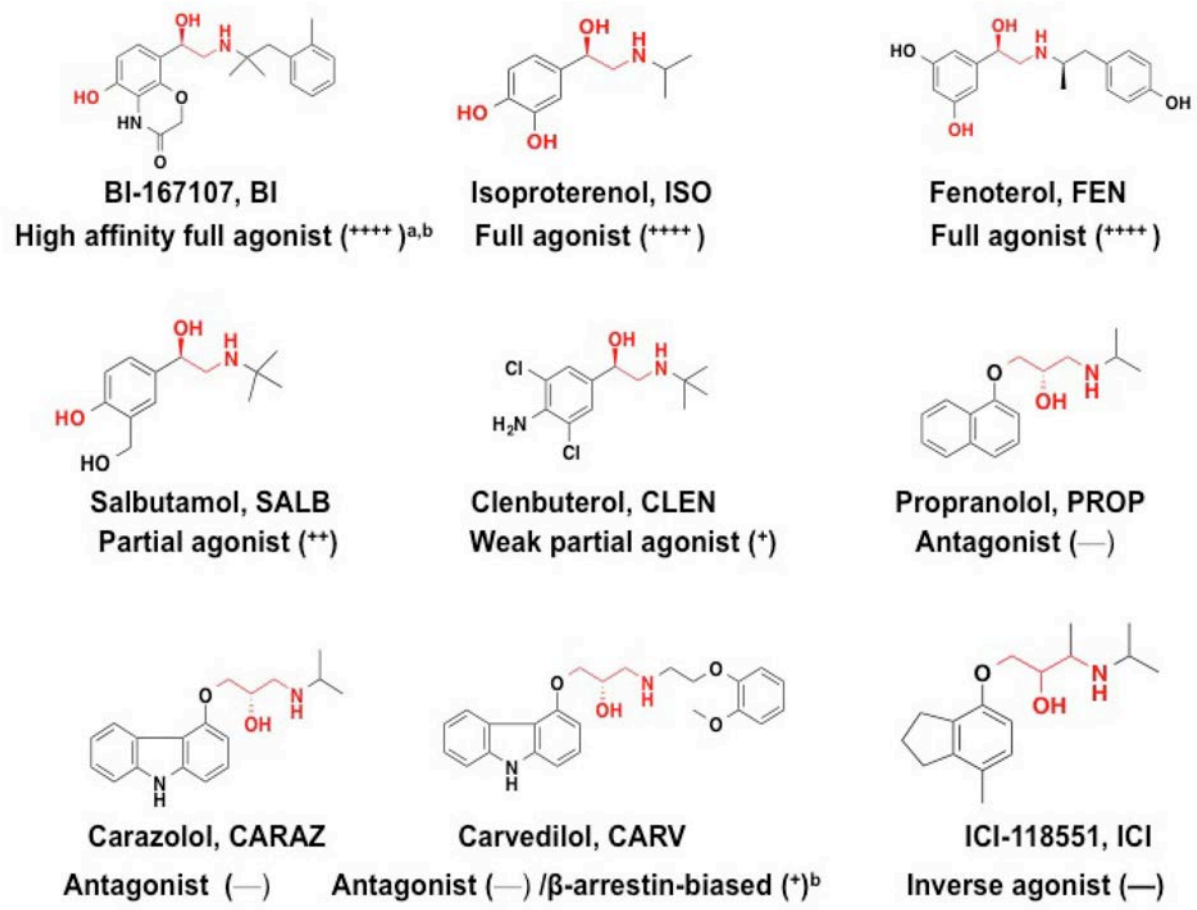

Supplementary Figure 6: Chemical structures of β_2AR ligands used in this study. Nine structurally and functionally distinct β-adrenoceptor ligands are shown. Qualitative functional properties of the ligands expressed relative to maximal stimulations (++++) and inhibition (–) of receptor activity: ($^{++++}$) Full agonists (BI, ISO, and FEN); ($^{++}$) a partial agonist (SALB); ($^{+}$) a weak partial agonist (CLEN); and four ($^{-}$) antagonists and ($^{-}$) inverse agonists (PROP, CARAZ, CARV, and ICI). The superscript "a" denotes a "super" high-affinity agonist with extremely slow off-rate while "b" denotes modestly biased ligands towards β-arrestin-dependent signaling pathways.

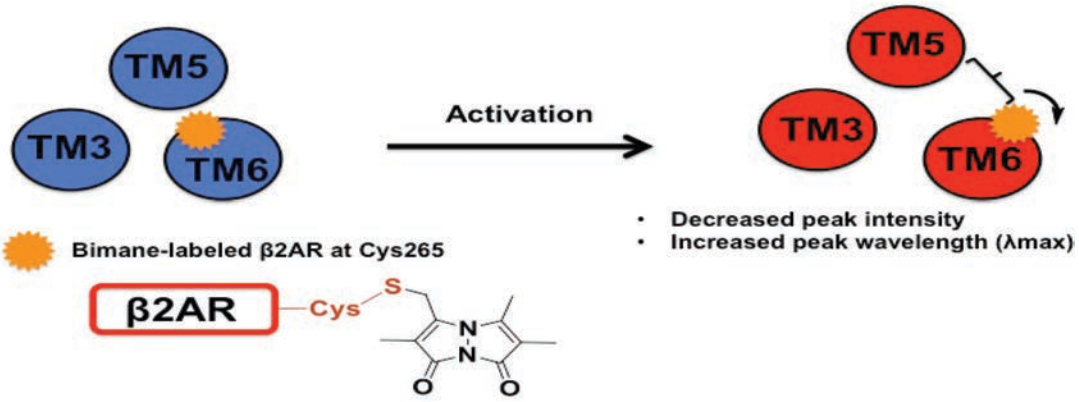

Supplementary Figure 7: Bimane fluorescence quenching measurement to monitor agonist dependent conformational rearrangements at TM6 of the β_2AR. Shown on the left side is a cartoon diagram view of cytoplasmic face of β_2AR with three transmembrane domain helices (TM3, TM5 and TM6). The orange denotes fluorescent probe bimane label, an environmentally sensitive fluorophore also shown by the chemical structure covalently attached via the thiol group of C265 (at TM6) after reaction with monobromobimane (mBrB). The probe enables direct monitoring of agonist-induced receptor conformational changes via TM6 movement (denoted by the red colored TMs on the right side) from a hydrophobic environment (a cavity between TM3, TM5, and TM6 shown in blue) to a more polar or solvent-exposed position as a decrease in fluorescence intensity and red-shift in emission λmax.

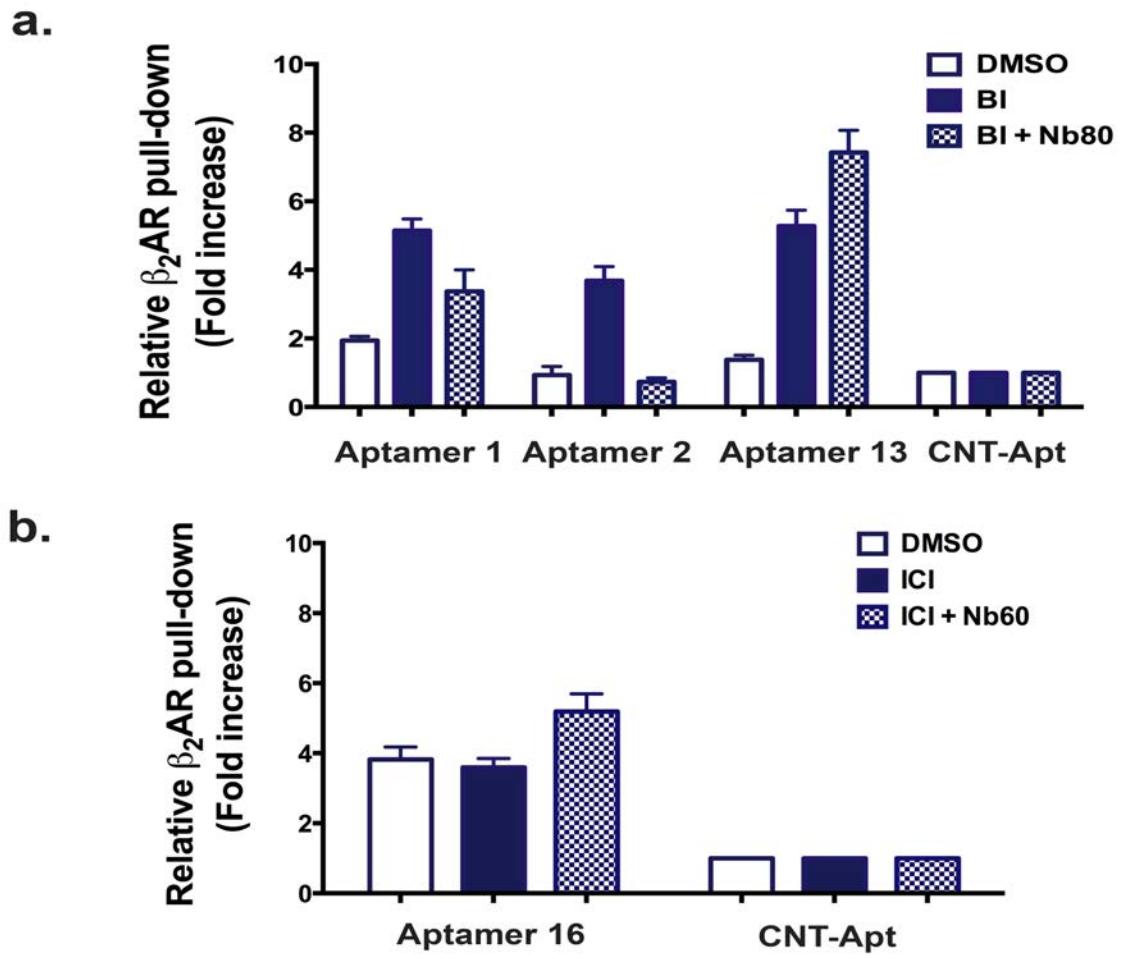

Supplementary Figure 8: Evaluation of binding mode and epitope of RNA aptamers using β_2AR specific allosteric modulator nanobodies (**a**,**b**) Bar graphs summarizing the ability of β_2AR nanobodies, Nb80 (**a**) or Nb60 (**b**) to compete with the interaction between aptamers (A1, A2, A13 or A16) and β_2AR. The *y*-axis shows binding of β_2AR to aptamers in presence or absence of β_2AR nanobodies: data normalized as fold increase of β_2AR binding detected in the presence control aptamer. The competition pull-down experiments were performed by pre-incubating 10 μM of competitors (Nb80 or Nb60) with 500 nM β_2AR (in presence or absence of ligands) and applied onto the immobilized biotinylated aptamer (2 μM) on NeutrAvidin beads. Shown in (**a**) are results for binding of aptamer A1, A2, or A13 with β_2AR in the absence (white) or presence of full agonist BI167107 (navy-blue), and combinations of BI167107 with Nb80 (white and navy-blue boxes). Shown in (**b**) are results for binding of aptamer A16 with β_2AR in the absence (white) or presence of inverse agonist ICI-118,551 (navy-blue), and combinations of ICI-118,551 with Nb60 (white and navy-blue boxes). Data are means from at least three independent experiments; error bars represent s.e.m.

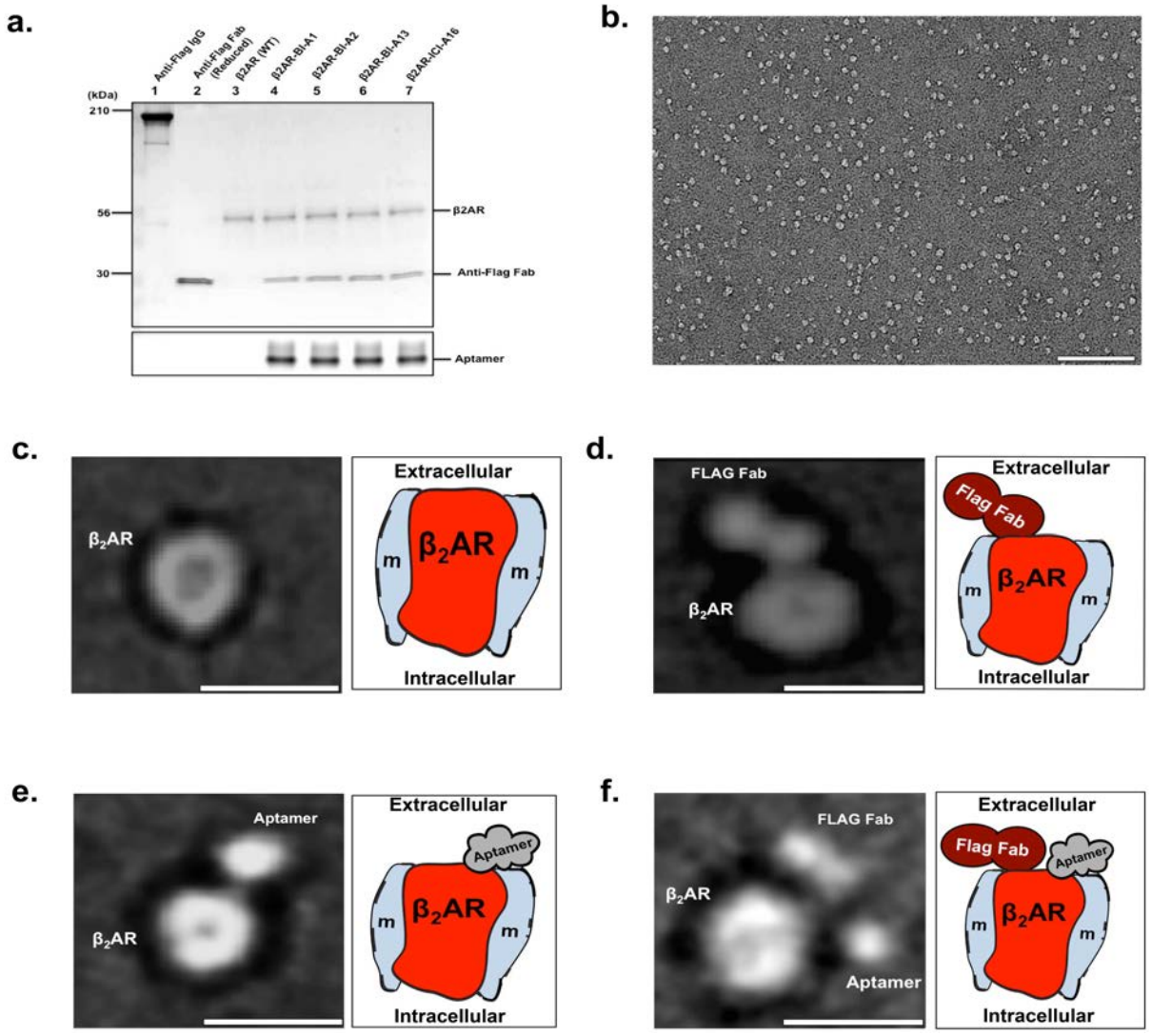

Supplementary Figure 9: Negative stain electron microscopy (EM) analysis of the β_2AR-aptamer complexes. (**a**) Anti-Flag Fab and affinity purification of β_2AR-aptamer-Fab complexes. SDS-PAGE analysis of β_2AR-aptamer-Fab complexes. Lane 1, anti-FLAG M1 antibody IgG; Lanes 2 anti-FLAG M1 Fab (reduced form); Lane 3: β_2AR; lanes 4-7: β_2AR-aptamer-Fab complexes (with A1, A2, A13 and A16, respectively) prepared by affinity chromatographic purification on neutravidin beads followed by elution using free biotin. Anti-FLAG Fab was obtained from purified IgG by papain digestion (see online **Methods**). Shown on the lower section of the panel are ethidium-bromide stained biotinylated aptamers resolved in TBE gels. Sample compositions are also indicated above the image and identity of the complex bands on its side. (**b**) Representative raw EM image of negative-stained β_2AR-aptamer (A2) complexes. Scale bar is 25 nm. (**c-f**) EM characterization of purified β_2AR:aptamer-Fab complexes. Shown on the left side of each panel are negative-stain two-dimensional (2D) class average particles: β_2AR alone (**c**), anti-FLAG Fab antibody-labeled-β_2AR (**d**), β_2AR in complex with a representative aptamer (**e**) and anti-FLAG Fab antibody-labeled-β_2AR in complex with the representative aptamer (**f**). Scale bar is 10 nm. Shown on the right side of each panel are cartoon representations for the components of the architecture of the complexes shown under the 2D class average images (β_2AR in red; detergent micelle labeled with "m" in light-gray; anti-FLAG Fab antibody in dark-red; the representative aptamer in gray).

Supplementary Table 1 | Kinetic profiles of aptamers and their binding ability to active and inactive β_2AR

	Aptamer A1		Aptamer A2		Aptamer A13		Aptamer A16	
	β_2AR: BI167107[d]	β_2AR:ICI-118,551[e]	β_2AR: BI167107	β_2AR:ICI-118,551	β_2AR: BI167107	β_2AR:ICI-118,551	β_2AR: BI167107	β_2AR:ICI-118,551
K_d (nM)[a]	42.0 ± 2.3	—[f]	258.5 ± 0.5	—	30.4 ± 2.4	—	—	93.1 ± 4.1
k_{on} ($10^4 M^{-1}S^{-1}$)[b]	1.0 ± 0.1	—	0.15 ± 0.02	—	1.5 ± 0.1	—	—	4.0 ± 0.2
k_{off} (10^{-4} S^{-1})[c]	4.2 ± 0.1	—	3.81 ± 0.54	—	4.6 ± 0.1	—	—	37.1 ± 2.1

[a]K_d is dissociation constant, given as the ratio of k_{off} to k_{on}; [b]k_{on} is association rate constant; and [c]k_{off} is dissociation rate constant. Each K_d value represents the mean affinity values ± s.e.m. of three independent experiments. [d] on β_2AR:BI167107 denotes an "active" conformation while [e] on β_2AR:ICI-118,551 an "inactive" conformation. [f] Denotes that dissociation constants could not be measured reliably due to poor signal to noise ratio.